Characterization of Retained Austenite in Case Carburized Gears and Its Influence on Fatigue Performance

Fouad B. Abudaia, J. Terry Evans and Brian A. Shaw

Carburized helical gears with high retained austenite were tested for surface contact fatigue. The retained austenite before testing was 60% and was associated with low hardness near the case's surface. However, the tested gears showed good pitting resistance, with fatigue strength greater than 1,380 MPa.

Detailed examination carried out on a gear that had been tested by contact on one flank on each tooth in a back-to-back test revealed that about 50% of the initial retained austenite was transformed to martensite during the test. Transformation was stress- or strain-assisted and was limited to a thin layer of 10 μm thickness or less at the surface. The increase in surface contact fatigue strength is attributed to the increased compressive residual stress and hardness in the mechanically transformed layer.

Introduction

High performance gears are case hardened to increase the hardness of the surface layer and thereby impart resistance to surface contact fatigue.

Table 1—Chemical composition of the investigated steel (percentage by weight).

C	0.17
Si	0.27
Mn	0.5
P	0.008
S	0.0039
Cr	1.66
Mo	0.28
Ni	1.5
Cu	0.15
Sn	0.011
Al	0.023
N	0.007
V	0.004

Table 2—Helical test gear dimensions.

Gear Property	Value
Helix angle (degrees)	30
Number of teeth	23
Module (mm)	6.0
Gear ratio	1:1
Center distance (mm)	160
DIN quality	5
Face width (mm)	38
Base circle diameter (mm)	150.35
Addendum (mm)	6.0
Tip diameter (mm)	172.0
Root diameter (mm)	142.7
Base pitch error (μm)	7.0
Form error (μm)	8.5
Tip relief (μm/mm)	70 μm over 0.8 mm
Total error (μm)	9.5

Case carburizing is extensively used for this purpose in gears and bearings. Carburization of the case increases the carbon content to levels between 0.8% and 1%. Also, subsequent heat treatment is used to produce a tempered martensitic structure with some retained austenite.

A number of standard heat treatments in gear applications require the retained austenite to be in the range of 15–20%. On the other hand, in aerospace applications, other standards require the retained austenite to be reduced to less than 4% by sub-zero cooling.

Generally, the effect of retained austenite on fatigue is not entirely clear. Zaccone et al. (1989) showed that high levels of retained austenite increased fatigue strength in bending fatigue in the low- to medium-cycle regime but reduced fatigue strength in the high-cycle regime.

One explanation is: Retained austenite, being softer than tempered martensite, imparts a high level of fracture toughness, which is beneficial in the low-cycle fatigue regime, where much of the fracture life is taken up with Stage II crack growth. Relatively little information has been published on the effect of retained austenite on the surface contact fatigue performance of gears.

In this paper, we present the results of back-to-back tests on case carburized gears with high retained austenite contents. Despite the fact that the hardness of the material in the case was significantly lower than in gears with normal retained austenite contents, the pitting fatigue resistance of the high austenite gears is good. It is believed that stress-induced transformation of retained austenite to martensite in a thin layer close to the surface is responsible for the relatively good pitting fatigue resistance.

Method and Materials

The performance of helical test gears made from low alloy steel containing a high level of retained austenite in the carburized case was investigated. The chemical composition of the gear material prior to case carburization is given in Table 1. The dimensions of the gear are given in Table 2.

The contact fatigue SN curve for these gears was determined by testing in a recirculating power, back-to-back test rig. Gears are considered failed when 4% of the involute flank areas contain pits or when obvious fracture took place. The SN curve is compared with that of low alloy steel containing a normal amount of retained austenite as shown in Figure 1.

The loaded flank was run for 32 million cycles with a contact stress of 1,455 MPa. The contact stress is the maximum stress operating in the area of contact between the involute flanks.

After the fatigue tests were conducted, a gear, which was run by contact of one flank of each tooth, was selected for examination. Teeth from the selected gear were removed, and tests were carried out on both the run and the un-run flanks.

Microhardness profiles on tooth cross sections were carried out with a 300 g load. The first indentation was taken at a distance of 50 µm from the surface. Retained austenite was measured by X-ray diffraction with a K_α radiation beam using AST-Stresstech's Xstress 3000 residual stress analyzer. Profiles up to a depth of 50 µm were made on both flank sides.

The Xstress 3000 residual stress analyzer was also used for residual stress measurements. Measurements were made on two orthogonal directions, the longitudinal direction or grinding direction and the direction transverse to the grinding direction. Note that the gears are ground in a direction parallel to the axis of the gear. The direction parallel to the grinding direction will be referred to as the 0° direction and the direction normal to this as the 90° direction. Profiles of the residual stresses in the martensite and the austenite phases were obtained to a depth of 50 µm.

Vickers macrohardness was used to measure the hardness of the run and un-run surfaces. One tooth was cut into two parts. Both parts were tested in the same manner, except that one part was tested after the removal of a 10 µm layer by etching. Loads of 1 kg, 2.5 kg, 5 kg and 10 kg were used on each side. The penetration depth of the indentor decreases as the testing loads decrease. Under smaller loads, the test could be confined to layers near to the surface. In addition, microhardness profiles were obtained in metallographic sections of the gear teeth.

In order to obtain more evidence for the changes that took place at and near the surface, optical microscopy examination was carried out on a metallographic section of a cut tooth.

Results

The retained austenite and the microhardness profile for the un-run flank are shown in Figures 2 and 3, respectively. These figures show the high level of the retained austenite associated with the low hardness values at a depth down to 0.8 mm below the surface.

Figure 4 shows the retained austenite profile in the run flank side. The level of the retained austenite was substantially decreased at the surface and near the surface compared with the un-run flank. The change from 60% in the un-run flank to 34% in the run flank was limited to a shallow depth.

Figures 5a and 5b show the surface macrohardness measurements versus depth of indentation for the un-etched and the etched parts of the tested tooth, respectively. The depth of indentation was varied by changing the applied load between 1 and 10 kg. The hardness of the run and un-run flanks was clear-

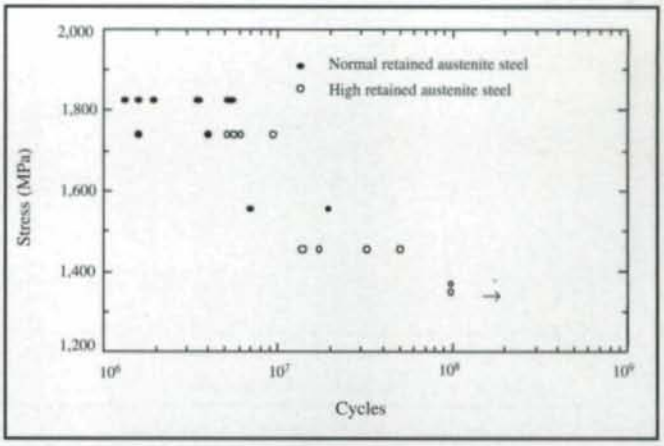

Figure 1—Stress vs. number of cycles for pitting fatigue in helical test gears. (The arrow indicates run out.)

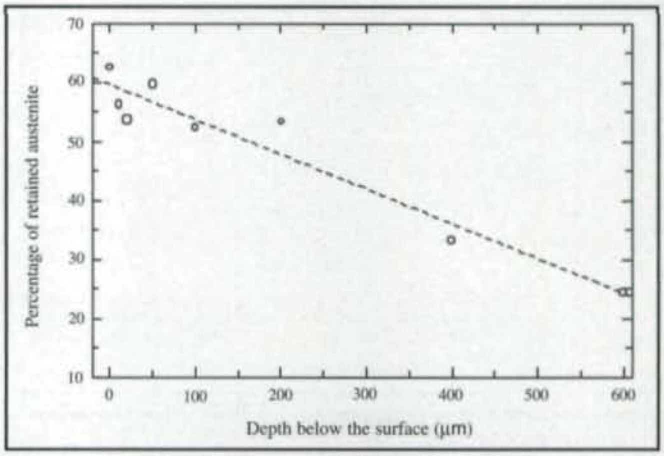

Figure 2—Retained austenite profile in the un-run flank.

Fouad B. Abudaia
is a doctoral student in the mechanical and systems engineering school at the University of Newcastle upon Tyne, United Kingdom. He holds a master's degree in material science and is performing research on the microstructure and fatigue strength of high performance gear steels.

J. Terry Evans
is a professor of materials engineering and acting head of the mechanical and systems engineering school in the University of Newcastle upon Tyne. He holds a doctorate in metallurgy and has published more than 200 papers in the field of deformation, fatigue and fracture of materials.

Brian A. Shaw
is a senior materials engineer with Design Unit, a part the mechanical and systems engineering school at University of Newcastle upon Tyne. A self-funded agency, Design Unit serves industry through research and consultancy, mainly in the field of gearing and mechanical power transmissions. Shaw holds a doctorate in materials engineering and has experience in metallurgical characterization of gear materials and fatigue failures. Also, he has consulted in areas related to residual stress, fatigue performance and material quality control in gear steels.

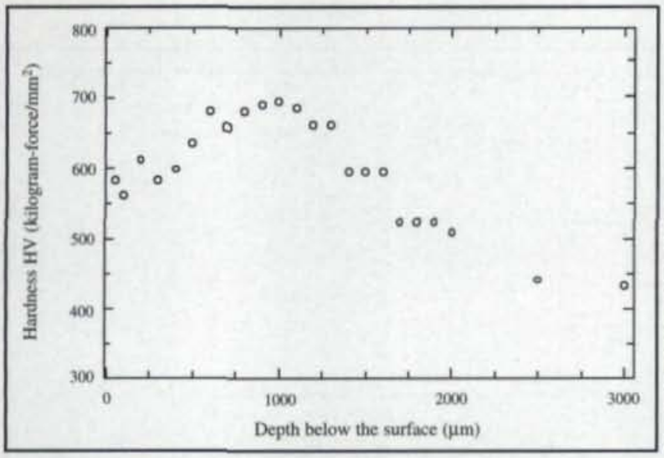

Figure 3—Microhardness profile for the un-run flank.

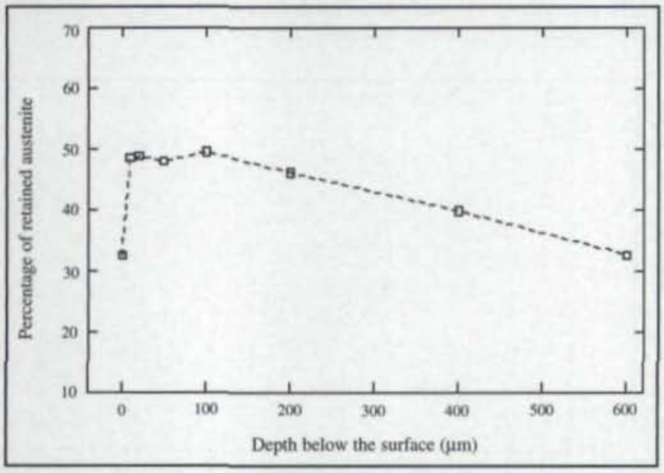

Figure 4—Retained austenite in the run flank after 32 million cycles at a surface contact stress of 1,455 MPa.

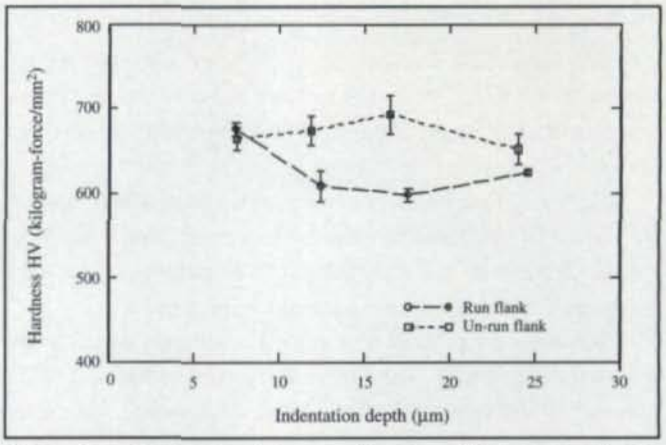

Figure 5a—Surface hardness as a function of indentation depth, before surface layer removal.

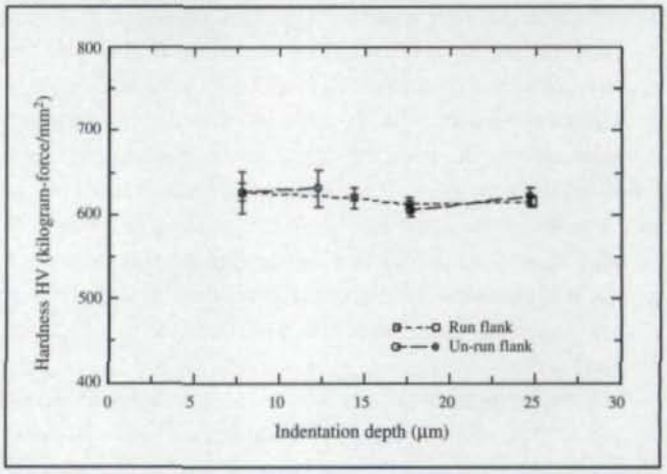

Figure 5b—Surface hardness as a function of indentation depth, showing the effect of surface layer removal.

ly different for the un-etched specimen (Fig. 5a). However, after etching 10 μm, the hardness values of the run and un-run flanks were sensibly the same (Fig. 5b).

Changes at shallow depths were also noticed for residual stress measurements. Residual stress profiles were measured in the run and un-run flanks in both the martensite and the retained austenite. In addition, residual stresses were measured in the 0° and 90° directions. The results are shown in Figures 6a–6d.

Figures 6a and 6b compare the residual stress profiles in the martensite phase for the run and un-run flanks on the 0° and the 90° directions, respectively.

Residual stresses in the austenite phase on both flanks and directions are shown in Figures 6c and 6d.

In the martensite phase in the 0° direction, the run flank showed a large compressive stress at the surface, whereas the un-run flank exhibited only a small compressive stress. In the martensite in the 90° direction, the un-run flank showed a residual stress of just less than –400 MPa while the run flank showed a stress just greater than –500 MPa. At depths greater than 10 μm, there was little difference between the run and un-run flanks.

A greater difference in the residual stress distributions down to a greater depth was observed in the austenitie phase in the 0° direction (Fig. 6c). However, a smaller difference was observed in the 90° direction (Fig. 6d).

Microstructures near the run and un-run sides of the same tooth are shown in Figures 7a and 7b, respectively. The microstructure was typical of material with large austenite grain size. Plates of martensite were clearly visible within the austenite matrix. A higher martensite plate content was evident near the surface of the run flank. This supports the idea that stress-assisted or strain-assisted martensite transformation occurred during surface contact.

Discussion

The high retained austenite content in the case of the carburized gear teeth produces a relatively low hardness down to a depth of 0.5 mm (Figs. 2 and 3). Despite the substandard hardness level, the gears with high retained austenite have good pitting fatigue resistance, with strength greater than 1,380 MPa at 10^8 cycles. Certainly, if fully martensitic specimens were overtempered to produce a similar low hardness, one would expect to see a significantly reduced pitting fatigue strength.

The evidence from hardness tests, X-ray diffraction and metallographic examination suggests that the good fatigue resistance is due to either stress- or strain-induced martensite transformation in a thin layer near the surface of the run involute flanks.

Figure 6—Residual stress distribution in the martensite and austenite phases.

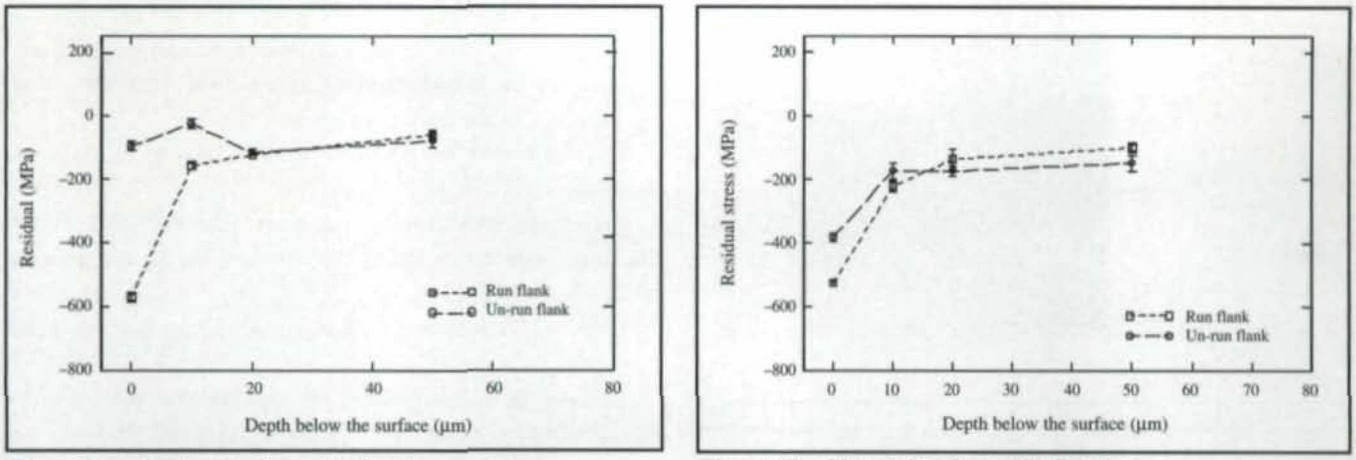

Figure 6A—Martensite phase, 0° direction

Figure 6B—Martensite phase, 90° direction

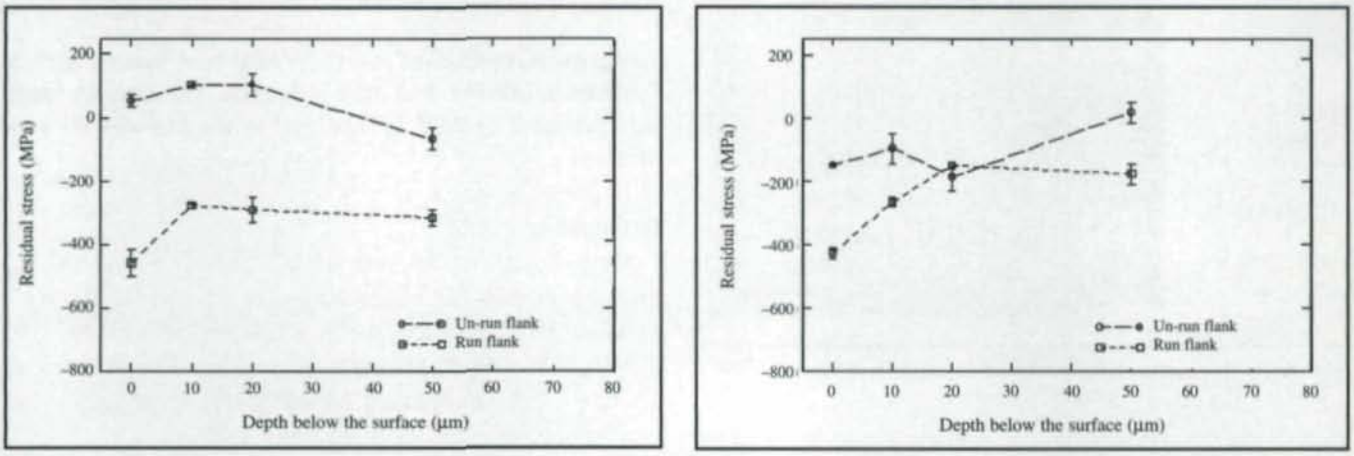

Figure 6C— Austenite phase, 0° direction

Figure 6D—Austenite phase, 90° direction

There is clear evidence that surface contact in the back-to-back tests reduces the retained austenite content at the surface by a factor of two. In the un-run flanks, the retained austenite content is of the order of 55–63% (Fig. 2). After cycling surface contact in the back-to-back tests, the retained austenite content at the surface was found to be reduced to the level of 30–35% (Fig 4).

The thin layer of contact-reduced retained austenite is of the order of 10 µm. This conclusion is supported by the surface hardness results in Figures 5a and 5b. In Figure 5a, the un-run surface shows a lower hardness than the run flank at penetration depths between 12 and 18 microns. Also in Figure 5a, at greater penetration depths, the hardness values converge. At the smallest penetration depth of 7 µm, the hardness values for the run and un-run flanks again converge. It is believed that, at the small indentor depth, the influence of strain hardening from grinding during manufacture is dominant, i.e. both run and un-run involute flanks were ground in the final stage of manufacture.

After the 10 µm surface layer was removed by etching, the hardnesses of run and un-run flanks were sensibly identical at all indentor penetration depths in the range 7–25 µm (Fig. 5b). This latter evidence supports the idea that significant hardness increases occur as a result of surface contact, but only to a depth of 10 µm or less. We note, however, that the relation between hardness and depth of indentation (Fig. 5a) does not give a direct relation between the measured hardness and the hardness gradient in the material surface layers, because the harder layer near the surface continues to influence measured hardness at penetration depths greater than the hardness of the layer.

The mechanism of stress- or strain-induced austenite to martensite transformation at the gear surface remains to be understood in detail. It is known that the transformation of retained austenite can be nucleated by externally imposed stress (or elastic strain) acting alone and by plastic strain (Olson, 1982). Maxwell et al. (1974) reported a different morphology for martensite produced by the aid of stress and plastic strain. In addition, stress-assisted and plastic-strain-assisted martensite formation operates over different temperature ranges. Stress-assisted martensite transformation occurs predominantly below a characteristic temperature M_s^{σ} while plastic-strain-assisted martensite occurs between M_s^{σ} and a higher temperature M_d. At temperatures above M_d, neither stress-assisted nor strain-assisted transformation of retained austenite occurs. Neu and Sehitoglu (1991) found for carburized 4320 steel that stress-induced transformation occurred between 22°C and 60°C.

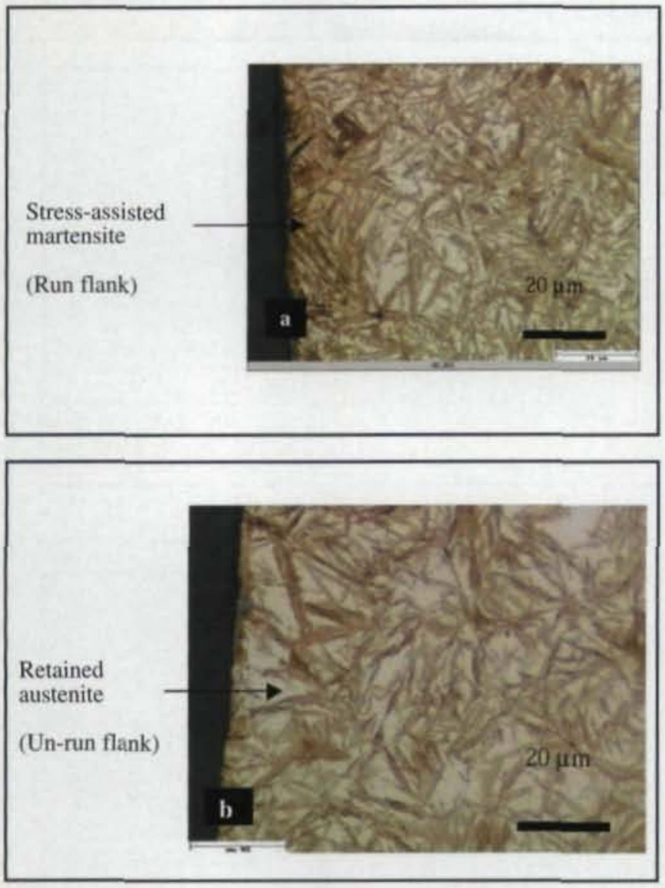

Figure 7—Microstructures in the run and un-run flanks.

A further observation is that compressive axial stress or hydrostatic stress suppresses the transformation, while axial or hydrostatic tension favors it. Thus, little strain-assisted transformation is observed when the plastic deformation occurs with a superimposed hydrostatic pressure, while the greatest amount of transformation occurred under axial tension (Neu and Sehitoglu, 1992). These observations are pertinent to the present results because the stress field produced by surface contact of the involute flanks is predominantly compressive.

The Von Mises stresses are less than the yield strength of the material for ideally smooth surfaces. Thus, any plastic deformation in the involute flanks must occur at the scale of the surface asperities. Even so, the superimposed hydrostatic stress is predominantly compressive, thereby acting to oppose strain-induced martensite transformation.

Surface contact had an effect on residual stresses only near the surface. As shown in Figure 6a, surface contact produced a significant surface residual compressive stress in the 0° direction. This is consistent with stress- or strain-induced martensite transformation, which is expected to produce residual compressive stress because of the associated 4% volume increase. On the other hand, it is believed that the surface residual stress is complicated by the treatment prior to testing. The last operation is surface grinding, and the different residual stresses in the 0° and the 90° directions in the un-run flanks (Figs. 6a and 6b) are typical of near-surface residual stresses produced by a grinding operation.

Conclusions

Gear materials made from steels with high levels of retained austenite showed high fatigue resistance and good performance.

Stress-assisted martensitic transformation occurred under the influence of the contact stresses.

Transformation was confined to a thin layer of about 10 (m in depth.

High compressive stresses are set up in the transformed layer due to constraint imposed by the austenite matrix and the core material.

Martensitic transformation caused the surface hardness to be increased.

Changes in microstructure, residual stresses and hardness were confined to a thin layer of about 10 µm in depth. These are beneficial changes from the surface fatigue point of view and resulted in improved performance. ○

This paper was presented at the 20th ASM Heat Treating Society Conference, held Oct. 9–12, 2000, in St. Louis, MO. Also, the paper was published by ASM International in the conference's proceedings.

References

1. Maxwell, P.C., A. Goldberg and J.C. Shyne. "Stress-Assisted and Strain-Induced Martensite in Fe-Ni-C Alloys," *Metallurgical Transaction*, Vol. 5, 1974, pp. 1305–1318.
2. Neu, R.W. and H. Sehitoglu. "Transformation of Retained Austenite in Carburized 4320 Steel," *Metallurgical Transaction*, Vol. 22A, 1991, pp. 1491–1500.
3. Neu, R.W. and H. Sehitoglu. "Stress-Induced Transformation in a Carburized Steel—Experiments and Analysis," *Acta Metallurgica Et Materialia*, Vol. 40, No. 9, pp. 2257–2268, 1992.
4. Olson, G.B. and M. Cohen. "A Mechanism for the Strain-Induced Nucleation of Martensitic Transformation," *Journal of Less Common Metals*, Vol. 28, pp.107–118, 1972.
5. Zaccone, M.A., J.B. Kelley and G. Krauss. "Strain Hardening and Fatigue of Simulated Case Microstructure in Carburized Steel," *Carburizing: Processing and Performance, ASM International*, Lakewood, Colorado, July 12–14, 1989.